

Optimization of feature extraction for the prediction of macromolecular interactions : OTE-24 Approach

1. Abstract

In the field of molecular biology, where every interaction between macromolecules is of crucial importance, analyzing the structural features of biological macromolecules remains a major challenge. Traditional feature extraction techniques from protein sequences often prove to be inefficient. The reliability of the extracted information is sometimes questionable due to the complexity and volume of the data involved. The volume and complexity of this biological data compel researchers in the field to turn to computational feature extraction techniques. Over the years, several computational methods have been proposed to accurately extract relevant and representative information from macromolecule sequences within these large datasets. However, these extraction techniques are sometimes impractical, and the relevance of the extracted information may be limited. In this study, we propose a large-scale feature extraction method based on the correlation analysis of two physicochemical properties of amino acids: hydrophobicity and hydrophilicity, as well as the correlation between amino acids. The results of this research, evaluated using databases commonly utilized in previous studies, show an accuracy improvement of over **2.58%** compared to existing methods.

Keywords : Molecular biology, Feature extraction, Physicochemical properties of amino acids, Hydrophobicity and hydrophilicity, Macromolecular interaction prediction

2. Introduction

In the drug development process, the study of interactions between biological macromolecules is crucial. This step is of paramount importance in the fields of biology, bioinformatics, and medical research. Biological macromolecules, such as proteins, nucleic acids, lipids, and polysaccharides, are the fundamental components of living organisms. Their interactions, whether at the cellular or macromolecular level, are responsible for regulating various biological processes, transmitting genetic information, and modulating immune responses, among other key functions [1]. Several high-throughput chemometric techniques, such as protein microarrays [2], Nuclear Magnetic Resonance (NMR) [3],[4], Biacore (Surface Plasmon Resonance) SPR [5], [6], and Isothermal Titration Calorimetry (ITC) [7], have been developed to detect these interactions. While these techniques have revealed numerous unknown interactions, they are often time-consuming and expensive. These constraints, combined with the volume and complexity of experimental data, have driven the development of computational models to predict large-scale macromolecular interactions.

Since the 1970s and 1980s, when computational techniques were introduced for detecting interactions between biological macromolecules, various approaches have been proposed to

41 predict macromolecule-macromolecule interactions (MMI) using datasets available in
42 biological databases. Several techniques, such as gene fusion [8],[9],[10], Archer FusionPlex
43 panels, QIAseq RNAscan, and OncoPrint Focus [11], 3D structural information [12], and
44 gene ontology and annotation [13],[14], have contributed to this goal.

45 However, these approaches are not universal due to their high computational complexity.
46 Their precision and reliability heavily depend on the information previously collected from
47 the datasets used during implementation. The practical implementation of these approaches,
48 as well as the practical information on gene annotation and ontology, is often incomplete for
49 several reasons. First, although the Gene Ontology database is widely used, it is not
50 exhaustive, and many annotations are incorrect or missing. This limits a comprehensive
51 understanding of gene functions and gene products in different biological contexts [15].
52 Furthermore, the 3D structure of many proteins remains unknown. A significant portion of
53 proteins has yet to be resolved using techniques such as X-ray crystallography or cryo-
54 electron microscopy, despite considerable efforts to determine these structures [16]. Finally,
55 macromolecule-macromolecule interactions (MMI) in many species are often rare and poorly
56 documented. This is partly due to the limitations of current experimental techniques, which
57 are costly and time-consuming, thereby restricting the amount of available data on MMIs [17].

58 Unlike amino acid data, which are widely available in biological databases, most of the
59 proposed approaches in the past use data extracted from sequences to study and predict
60 macromolecule interactions.

61 Several sequence-based approaches for macromolecule analysis have been proposed. For
62 example, the Biological Jaccard Index [16] measures the similarity between macromolecule
63 sequences. This method identifies k-mers (subsequences of length k) in each macromolecule
64 and calculates the Jaccard similarity between these sets. However, this method is sensitive to
65 variations (it performs less well for low sequence similarity) and does not account for
66 structural information, which may limit its accuracy for certain complex interactions. Another
67 approach is the ISLAND method, which uses various feature representations of
68 macromolecular sequences, including amino acid composition (AAC), the average features of
69 the BLOSUM-62 substitution matrix, Position Specific Scoring Matrix (PSSM) features, and
70 descriptors derived from the biophysical properties of amino acids to model evolutionary
71 relationships and physicochemical properties of macromolecules [18]. However, the diversity
72 of features used in this method increases computational complexity, and its accuracy depends
73 heavily on the quality of the data.

74 Another approach, the Stacked Autoencoder method, transforms macromolecular sequences
75 into numerical features using methods such as autocovariance and conjoint triad, then trains
76 an autoencoder to learn compact and informative representations of the sequences [19]. In
77 addition to sharing the same data dependency limitation as the ISLAND method, this
78 approach may suffer from overfitting.

79 N-gram-based approaches are also used for the analysis and prediction of interactions. These
80 approaches focus on analyzing macromolecule sequences as fixed-length (n-gram) or
81 variable-length segments [20]. The approach proposed by Kopoin et al. for predicting protein-
82 protein interactions uses bigrams, where $n = 2$. It examines consecutive pairs of amino acids
83 in the sequences. The physicochemical properties of hydrophobicity and hydrophilicity of

84 amino acids are used to create these bigrams. This method is also combined with the Position
85 Specific Scoring Matrix (PSSM), which provides information on the probability of amino acid
86 substitutions according to their position. This allows for the generation of an enriched matrix
87 that captures both the relationships between amino acids and contextual information. These
88 features are then used to train an artificial neural network, which improves the accuracy of
89 protein-protein interaction prediction. Although n-gram-based models effectively capture
90 local patterns, they often experience contextual information loss. These approaches are also
91 sensitive to the choice of n, as their performance varies depending on the size of the selected
92 n-grams.

93 In this study, we propose an approach that combines the amino acid correlation calculation
94 method proposed by Chou [21] with the bigram method proposed by Kopoin et al. in 2020
95 [20] to extract features from macromolecular sequences. In our research on macromolecule-
96 macromolecule interactions, we employ the Random Forest algorithm [22], [23] to effectively
97 learn the representations of macromolecule pairs. To evaluate the effectiveness of our model,
98 we applied it to a large dataset of macromolecule-macromolecule interactions from the work
99 of Vazquez et al. [24].

100 **3. Materials and Methods**

101 **3.1 General Overview**

102
103 This study relies on a dataset of macromolecular interactions from the Human Protein
104 Reference Database (HPRD), as described in the study by [25]. This reference database,
105 widely used by many researchers for predicting interactions between macromolecules, is
106 publicly accessible.

107 The developed approach focuses on extracting features from macromolecular sequences,
108 enabling the extraction of the physicochemical properties of amino acids. Random forests,
109 known for their robustness and efficiency in classification and pattern recognition, were used
110 to predict macromolecular interactions [26]. The effectiveness of this classification method
111 guided our choice of model, allowing us to achieve promising results [26], demonstrating a
112 significant improvement in the predictive accuracy of macromolecular interactions. A detailed
113 illustration of the process is presented in Figure 1.

114 **3.2 Dataset**

115
116 In this study, we focus on implementing a model based on macromolecular sequences to
117 predict macromolecule-macromolecule interactions (MMI). The dataset of macromolecular
118 interactions was derived from the Human Protein Reference Database (HPRD) [27]. To ensure
119 data quality, duplicates were removed from the carefully selected positive data. For the
120 construction of negative pairs, which represent non-interacting macromolecule pairs, the
121 authors [15] paired macromolecules located in distinct subcellular localizations, using the
122 observable macromolecular localization information available in version 57.3 of the Swiss-
123 Prot database (uniprot.org). In their approach, they excluded shorter sequences (fewer than 50
124 amino acids) as well as those with multiple localizations, ensuring a high level of
125 representativeness.

126 Our dataset includes a total of 36,630 positive interactions involving 9,630 different human
 127 macromolecules. To balance the dataset, we also selected 36,480 negative interaction pairs
 128 derived from 1,773 macromolecules [28], [29]. We also use datasets from Swiss-Prot [30], the
 129 Protein Data Bank (PDB) [31], BioGrid, and STRING [32] to compare the effectiveness of
 130 our method with other recent approaches in the field of MMI.

131 3.3 Random forest

132 Random Forest is a supervised learning algorithm that works by creating a collection of
 133 decision trees, where each tree is built from a random sample of the training data. This
 134 technique, known as bagging (Bootstrap Aggregating), allows for the creation of subsets of
 135 data from the original dataset X , where each subset S_i is a randomly drawn sample with
 136 replacement of size N .

$$S_i = \text{Sample}(X, N) \quad [1]$$

137 Each tree is then trained on a distinct sample, which enhances the robustness and accuracy of
 138 the model. In classification, each tree produces a prediction, and the final result is determined
 139 by a majority vote from the trees, as represented by:

$$\mathcal{H} = \text{mode}(h_1, h_2, h_3, \dots, h_T) \quad [2]$$

140 where h_t is the prediction of the t -th tree, and T is the total number of trees. In regression
 141 problems, the final prediction is the average of the tree predictions:

$$\mathcal{H} = \frac{1}{T} \sum_{t=1}^T h_t \quad [3]$$

142 One of the key concepts in Random Forest is the use of measures such as Gini impurity or
 143 entropy to determine the most appropriate splits in the trees.
 144 **Gini Impurity:** In binary classification, Gini impurity G measures the probability that an
 145 observation will be misclassified if it were randomly assigned according to the class
 146 distribution in the node. It is calculated using the formula :

$$G = 1 - \sum_{i=1}^C P_i^2 \quad [4]$$

147 where P_i is the proportion of instances belonging to class i , and C is the number of possible
 148 different classes that the target variable can take.
 149 Entropy (Alternative to Gini Impurity): Entropy is another measure of node homogeneity,
 150 often used with information gain. It is defined as :

$$H(S) = - \sum_{i=1}^C P_i \log_2(P_i) \quad [5]$$

151 These measures allow each tree to choose the features that provide the best splits by
 152 minimizing impurity or maximizing information.

153

154 Resistance to Overfitting and Feature Selection

155

156 Random Forest is also resistant to overfitting, particularly when the number of trees is
157 sufficiently large. It combines multiple weak models to create a more powerful one.
158 Additionally, Random Forest efficiently handles datasets with a large number of features.
159 Each tree in the forest uses a subset of these features, randomly selected at each node, which
160 increases diversity between the trees. The importance of features can be measured by the
161 average reduction in impurity (Gini or Entropy) for each feature X_j across all trees, according
162 to the following formula:

$$I(X_j) = \frac{1}{T} \sum_{t=1}^T \Delta G_t(X_j) \quad [6]$$

163 where $\Delta G_t(X_j)$ is the impurity reduction for tree t when the feature X_j is used.

164 **Key Hyperparameters of Random Forest:** Random Forest has several hyperparameters that
165 directly influence its performance. These parameters include:

- 166 • **The number of trees (`n_estimators`) :** This is the total number of trees in the forest. A
167 higher number of trees tends to improve overall accuracy, although it also increases
168 computation time. The relationship between the number of trees and model accuracy
169 can be approximated by:

$$Accuracy_{RF} \approx f(n_{estimators}) \quad [7]$$

- 170 • **Maximum depth (`max_depth`):** This controls the depth of each tree. A greater depth
171 allows for capturing complex relationships in the data but may lead to overfitting.
- 172 • **Number of features selected at each split (`max_features`):** This parameter
173 determines how many features are available for each tree when making decisions. A
174 restricted selection promotes diversity among the trees, thus reducing the risk of
175 overfitting.

176 4. Proposed Feature Extraction Approach

177 This section explains our feature extraction approach, named OTE-24. This approach is
178 inspired by the Bi-gram method proposed by Kopoin et al. [20] and the method for calculating
179 amino acid correlation features by Chou in the APAAC method [21]. The computational
180 models proposed in the literature require learning relevant and representative features of
181 sequence pairs from the training dataset in order to perform prediction tasks on the test
182 dataset.

183 Kopoin et al.'s approach extracts protein features using physicochemical properties in the
184 form of bigrams. It involves calculating the physicochemical distance values for each amino
185 acid sequence in the dataset, forming an $L \times 20$ matrix represented by C , where L is the
186 length of the amino acid sequence, and creating a bigram feature vector from the data matrix
187 for training. It uses the ANN classifier to predict protein interactions. Chou's Amphiphilic

188 Pseudo Amino Acid Composition (APAAC) method is an improvement over the Pseudo
 189 Amino Acid Composition (PseAAC) method, designed to capture both hydrophobic and
 190 hydrophilic features of amino acids in protein sequences [33]. This method accounts for both
 191 the order of amino acids and the physicochemical properties of proteins, which is crucial for
 192 applications such as protein function prediction or their interaction with other
 193 macromolecules. APAAC is calculated using two key properties of amino acids:
 194 hydrophobicity and hydrophilicity. These values are integrated into a correlation function,
 195 which measures the similarity between two amino acids, and are then used to generate
 196 additional descriptors related to the amino acid sequence order [34].

197 **4.1 Description of Our Approach**

198 Our approach uses the bigram method and the pseudo-amino acid composition with
 199 autocorrelation (APAAC) method to generate feature vectors from macromolecular
 200 sequences, thereby facilitating the prediction of interactions between biological
 201 macromolecules. First, bigrams are calculated to extract local interactions between
 202 consecutive residues based on their physicochemical properties, such as hydrophobicity and
 203 hydrophilicity, resulting in a 400-value vector. Then, the APAAC amino acid correlation
 204 calculation method is applied to integrate global correlations on a larger scale, adding $2 \times 2 \times \lambda$
 205 additional values to capture long-distance interactions. λ represents the interaction length,
 206 defining the range of interactions between amino acid residues. This process results in a final
 207 vector of $800 + 2 \times 2 \times \lambda$ values for each sequence, providing a rich and detailed representation
 208 of the structural and functional features of macromolecules.

209 Our general formula is as follows:

$$A_t = \begin{cases} \sum_{i=1}^{L-1} C_{k,i} \cdot C_{k+1;j} , & \text{with } 1 \leq i \leq 20 \text{ and } 1 \leq j \leq 20 \\ \frac{N(t)}{1 + \varphi \sum_{t=1}^L f_t} , & \text{with } 1 \leq t \leq L \end{cases} \quad [8]$$

210 Where A_α is the numerical value or feature of the amino acid A at position α in the
 211 macromolecular sequence, $N(t)$ is the number of occurrences of amino acid t in the sequence.
 212 L is the length of the macromolecule sequence. φ is the weight parameter that adjusts the
 213 influence of the physicochemical properties of the amino acids relative to their base
 214 frequency, thus balancing the contribution of residue interactions and the simple composition
 215 of the macromolecular sequence. f_l is the correlation function based on the physicochemical
 216 properties of the amino acids, calculated as follows:

$$f_l = \frac{1}{N-l} \sum_{j=1}^{N-l} H_1(j) \cdot H_1(j+l) + H_2(j) \cdot H_2(j+l) \quad [9]$$

217 N is the length of the macromolecule sequence, i.e., the total number of amino acid residues.
 218 H_1 and H_2 are the values of hydrophobicity and hydrophilicity properties, respectively. They
 219 are used to represent the similarity or difference between amino acids at two positions j and
 220 $j+l$. 1 is the offset between two indices in the macromolecule sequence. If $l=1$, we study
 221 interactions between adjacent amino acid residues, and for $l>1$, we consider interactions
 222 between residues separated by a specific number of positions in the sequence, allowing us to
 223 capture long-range interactions.

224 Here, $C_{i,j} = \frac{1}{i}D(R_i, R_j)$ with $i = 1 \dots 20$ and $j = 1 \dots 20$ [10] .

225 The $C_{i,j}$ represent the physicochemical distance values between amino acids in the sequence.
226 Specifically, $C_{k,i}$ is the physicochemical distance value at position k for amino acid i . $C_{k+1,j}$ is
227 the physicochemical distance value at position $k+1$ for amino acid j . These values are used to
228 calculate the transition frequency between amino acids i and j in the sequence. L is the length
229 of the macromolecule sequence. $\frac{1}{i}$ is the weighting function for rank i .

$$D(R_i, R_j) = \frac{1}{2} \left\{ [h_1(R_j) - h_1(R_i)]^2 + [h_2(R_j) - h_2(R_i)]^2 \right\} \quad [11]$$

230 R_i and R_j are the amino acid residues of rank i and j , respectively. Then, $h_1(R_j)$ and $h_1(R_i)$ are
231 the respective numerical values of the hydrophobicity of residues R_i and R_j , and $h_2(R_j)$ and
232 $h_2(R_i)$ are the values of hydrophilicity for R_i and R_j . These values are calculated using the
233 following formulas:

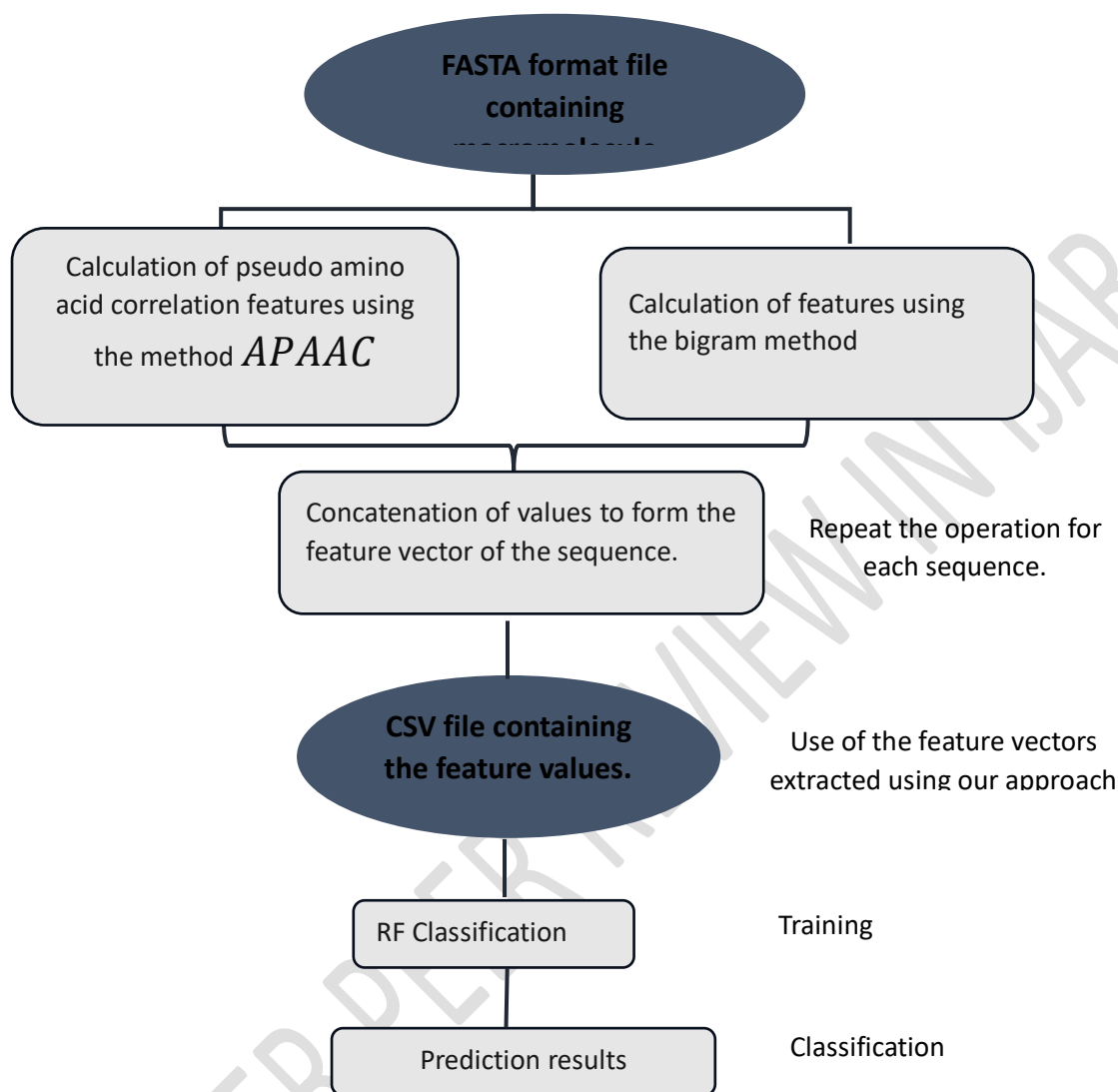
$$\begin{cases} h_1(R_i) = \frac{H_1^0(R_i) - \sum_{k=1}^{20} H_1^0(\mathbb{R}_k)/20}{\sqrt{\sum_{t=1}^{20} [H_1^0(R_i) - \sum_{k=1}^{20} H_1^0(\mathbb{R}_k)/20]^2/20}} \\ h_2(R_i) = \frac{H_2^0(R_i) - \sum_{k=1}^{20} H_2^0(\mathbb{R}_k)/20}{\sqrt{\sum_{t=1}^{20} [H_2^0(R_i) - \sum_{k=1}^{20} H_2^0(\mathbb{R}_k)/20]^2/20}} \end{cases} \quad [12]$$

234 The \mathbb{R}_k values range from 1 to 20 and represent the 20 natural amino acids according to the
235 alphabetical order of their one-letter codes: A, C, D, E, F, G, H, I, K, L, M, N, P, Q, R, S, T, V,
236 W, and Y.

237

238
 239
 240
 241
 242
 243
 244
 245
 246
 247
 248
 249
 250
 251
 252
 253
 254
 255
 256
 257
 258

4.2 The architecture (flowchart)



259 **Figure 1** : Algorithmic diagram of the OTE-24 approach

260 In our study, we undertook a methodical approach to extract meaningful features from amino
 261 acid sequences. First, for each sequence, we calculated the physicochemical distance values,
 262 which allowed us to construct an $L \times 20$ matrix, where L is the length of the sequence. Next,
 263 we determined the pseudo-amino acid components specific to each amino acid, which are
 264 essential for capturing important information about the sequence.

265 At the same time, we generated a bigram feature vector from the data of the matrix C. These
 266 bigram vectors capture the local relationships between amino acids, taking into account
 267 successive pairs, enriching the sequence representation. These two vectors (the APAAC
 268 component vector and the bigram vector) were then concatenated to form a global vector that
 269 captures both the physicochemical characteristics and sequential relationships.

270 Finally, this global vector was fed into a classifier based on the Random Forest algorithm for
 271 the learning and prediction phases.

272 4.3 The evaluation metrics of the model.

273 We use widely recognized measurement criteria in the literature [35], [36] to evaluate the
274 performance of our proposed approach and compare it with other existing models. These
275 criteria include accuracy (Acc), precision (Pre), sensitivity (Sen), negative predictive value
276 (NPV), F1 score (F1), and Matthews correlation coefficient (MCC). Accuracy (Acc) assesses
277 the overall proportion of correct predictions made by the model, including both correctly
278 predicted positives and negatives. Precision (Pre) measures the proportion of positive
279 predictions made by the model that are actually correct, indicating its ability to limit false
280 positives. Sensitivity (Sen), also called recall, evaluates the proportion of true positives
281 detected by the model among all the actual true positives, which is crucial for identifying all
282 real interactions. Negative predictive value (NPV) quantifies the proportion of true negatives
283 among all negative predictions, ensuring that the model minimizes false negatives. The F1
284 score (F1) is a harmonic mean of precision and sensitivity, offering a balance between the
285 ability to detect true positives and avoid false positives. The Matthews correlation coefficient
286 (MCC) evaluates the correlation between the model's predictions and the actual observations,
287 taking into account all cells of the confusion matrix to provide a global assessment of the
288 model's performance. These metrics allow us to assess the model's ability to effectively
289 discriminate between interactions and non-interactions between biological macromolecules,
290 which is crucial for the reliability and practical usefulness of the model in biomedical research
291 [27]. The AUROC and AUPRC measures are essential for evaluating models predicting
292 interactions between biological macromolecules. AUROC assesses the model's ability to
293 distinguish true interactions from non-interactions by integrating the ROC curve, which
294 represents sensitivity versus 1 - specificity across all classification thresholds. A high AUROC
295 score near 1 indicates strong discrimination capability. In contrast, AUPRC focuses on
296 precision and recall across different classification thresholds, with a high value indicating
297 good precision and high recall, both of which are essential for applications requiring accurate
298 detection of biological interactions. These metrics provide a comprehensive evaluation of the
299 model's performance by integrating both its discriminative ability and its precision across the
300 full range of decision thresholds for interactive and non-interactive macromolecules. The
301 formulas for calculating these measures are:

302 ▪ **Accuracy (Acc)**

303
$$AAC = \frac{TP+TN}{TP+TN+FN+FP} \quad [13]$$

304
305 ▪ **Precision (Pre)**

306
$$Pre = \frac{TP}{TP+FP} \quad [14]$$

307 ▪ **Sensitivity (Sen) (Recall)**

308
$$Sen = \frac{TP}{TP+FN} \quad [15]$$

309 ▪ **Negative Predictive Value (NPV)**

310
$$NPV = \frac{TN}{TN+FN} \quad [16]$$

311 ▪ **Score F1 (F1)**

312
$$F1 = 2 \cdot \frac{Pre \cdot Sen}{Pre + Sen} \quad [17]$$

313 ▪ **Specificity (Spe)**

314
$$Spe = \frac{TN}{TN+FP} \quad [18]$$

- 315 ▪ **Matthews Correlation Coefficient (MCC)**

316
$$MCC = \frac{TP*TN-FP*FN}{\sqrt{(TP+FP)*(TP+FN)*(TN+FP)*(TN+FN)}} \quad [19]$$

- 317 ▪ **Area Under the ROC Curve (AUC-ROC)**

318
$$AUCROC = \int_0^1 Sen(FRP^{-1}(t))d(1 - Spe(FRP^{-1}(t))) \quad [20]$$

319

320 Where $FRP^{-1}(t)$ is the inverse function of the false positive rate for a
321 decision threshold t .

- 322 ▪ **Area under the precision-recall curve (AUPRC)**

323
$$AUPRC = \int_0^1 Pre((t))d(Recall) \quad [21]$$

324 **True Positives (TP):** Represent the interactions between macromolecules that we correctly
325 predicted. For example, when we predict that an interaction occurs between two proteins, and
326 this prediction is confirmed by experimental data, it constitutes a true positive.

327 **True Negatives (TN):** Correspond to pairs of macromolecules for which we correctly
328 predicted that no interaction occurs. For example, if we predict that a specific enzyme does
329 not interact with a particular substrate, and this is confirmed by the data, it is counted as a true
330 negative.

331 **False Positives (FP):** Are situations where we incorrectly predicted that an interaction
332 occurred between two macromolecules, while in reality, it does not occur. For example, if our
333 model suggests that protein A interacts with protein B, but this interaction is not observed
334 experimentally, it constitutes a false positive.

335 **False Negatives (FN):** Occur when our model fails to detect an interaction that actually exists
336 between two macromolecules. For example, if two macromolecules do interact but our model
337 does not predict this interaction, it is counted as a false negative.

338 By analyzing these categories (**TP, TN, FP, FN**), we evaluate the overall performance of our
339 prediction models. This evaluation is crucial for refining our approaches and improving the
340 accuracy of our results in predicting interactions between biological macromolecules.

341 5. Results

342

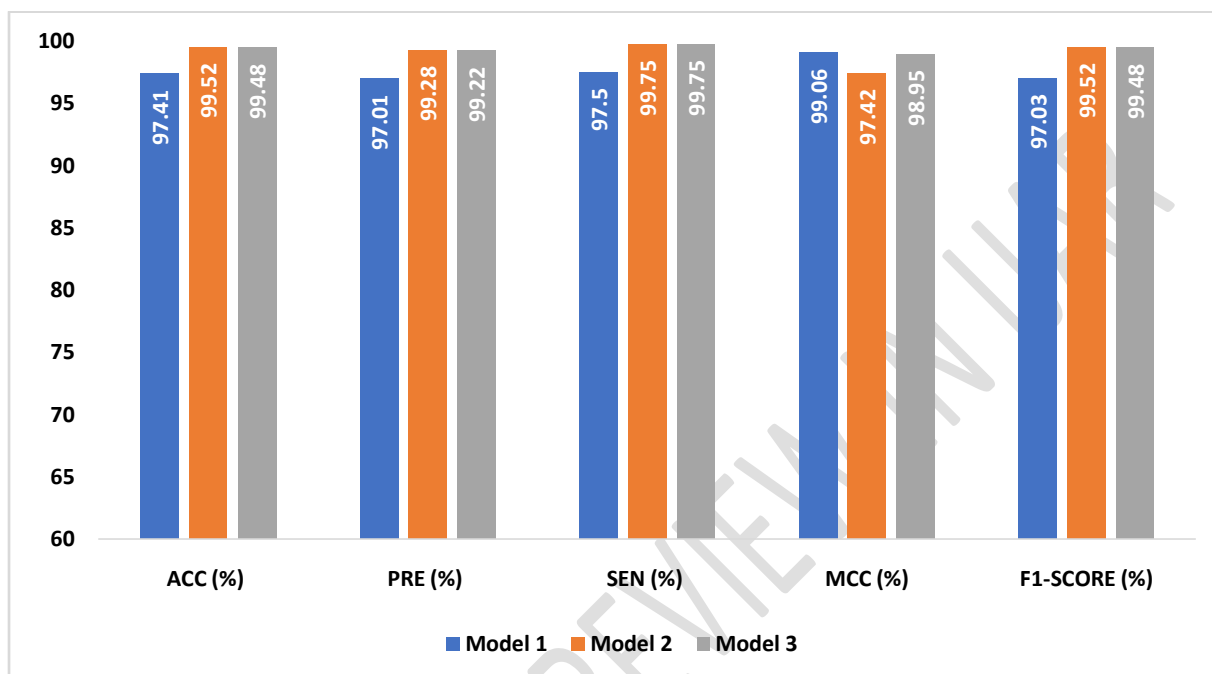
343 In this section, we present the results obtained and compare them with those reported by other
344 researchers using different methods. For this project, we developed a method based on
345 sequence analysis to predict interactions between biological macromolecules. Unlike some
346 previous studies, we used Python version 3.11.6 with JupyterLab in the Anaconda
347 environment version 2.5.4, which allowed us to benefit from improved dependency
348 management and a powerful interactive development environment.

349 5.1 Predictive performance of the proposed approach

350

351 In the predictive part, we used the same principle of splitting our datasets to train the chosen
352 model with our extracted data. These features, in the form of numerical vectors, are used as
353 input for our OTE-24 model. We performed 5-fold cross-validation on our reference dataset,
354 which allowed us to train 3 different models. The results obtained are presented in Figure 2.

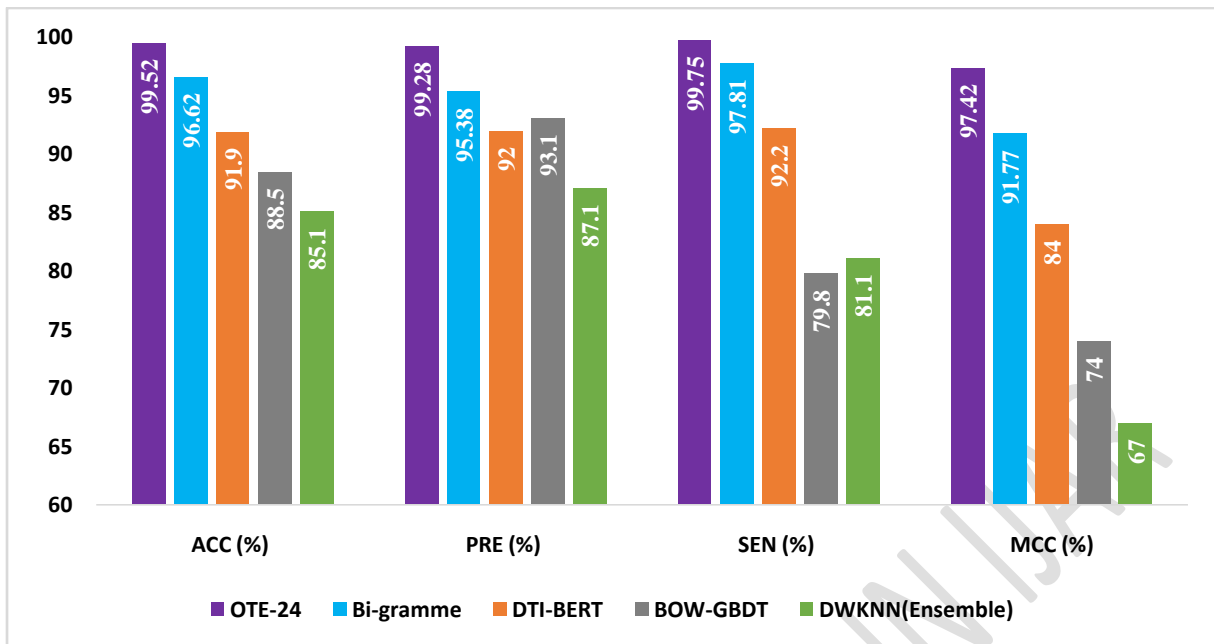
355 Model 2 showed the best performance with a precision of 99.29%, an accuracy of 99.52%, a
 356 recall of 99.75%, an F1-score of 99.52%, and an area under the ROC curve (ROC AUC) of
 357 99.99%. On average, the performances are 98.83% for precision (PRE), 99.4721% for
 358 accuracy (ACC), 98.83% for recall (SEN), 98.67% for the F1-score, and 83.67% for the ROC
 359 AUC. The high values of these different metrics, all above 98% except for the ROC AUC,
 360 indicate excellent predictive performance.



361
 362 **Figure 2** : Performance comparison of the three models trained on the HPRD database.

363 5.2 Comparison of our approach with other techniques

364
 365 We compared our method with several other commonly used feature extraction techniques
 366 from the literature, applied to the same human dataset. These techniques include the bigram
 367 method [20], DWKNN (Ensemble) [37], BOW-GBDT [38], and DTI-BERT [39]. The
 368 comparison is based on various evaluation metrics. Figure 3 highlights these different
 369 comparison metrics between our approach and the approaches from the literature.



370

371 **Figure 3:** Comparison of the OTE-24 model with models from the literature

372 We compared our method with several other commonly used feature extraction techniques
 373 found in the literature, applied to the same human dataset. These techniques include the bi-
 374 gram method [20], DWKNN (Ensemble) [35], BOW-GBDT [36], and DTI-BERT [37]. The
 375 comparison is based on various performance metrics. Figure 3 highlights the differences in
 376 these metrics between our approach and those from the literature.

377 This comparison revealed an accuracy (ACC) of 96.62%, 91.90%, 88.50%, and 85.10% for the
 378 bi-gram, DTI-BERT, BOW-GBDT, and DWKNN (Ensemble) methods, respectively,
 379 compared to 99.52% for our approach (OTE-24). This represents an improvement of 2.90%,
 380 7.62%, 11.02%, and 14.42%, respectively.

381 Regarding precision (PRE), the rates are 95.38%, 92%, 93.10%, and 87.10% for the bi-gram,
 382 DTI-BERT, BOW-GBDT, and DWKNN (Ensemble) methods, respectively, compared to
 383 99.28% for our approach. This corresponds to an improvement of 3.90%, 7.28%, 6.18%, and
 384 12.18%, respectively.

385 For sensitivity (SEN), we observed rates of 97.81%, 92.20%, 79.80%, and 81.10% for the bi-
 386 gram, DTI-BERT, BOW-GBDT, and DWKNN (Ensemble) methods, respectively, compared
 387 to 99.75% for our approach. This results in an improvement of 1.94%, 7.55%, 19.95%, and
 388 18.65%, respectively.

389 As for the Matthews Correlation Coefficient (MCC), the rates are 91.77%, 84%, 74%, and
 390 67% for the bi-gram, DTI-BERT, BOW-GBDT, and DWKNN (Ensemble) methods,
 391 respectively, compared to 97.42% for our approach. This represents an improvement of
 392 5.65%, 13.42%, 23.42%, and 30.42%, respectively.

393 Our analysis shows that our technique surpasses the bi-gram method by at least 1.94%,
 394 DWKNN (Ensemble) by 12.18%, BOW-GBDT by 6.18%, and the DTI-BERT method by
 395 7.28% on all the studied metrics.

396 In the study of macromolecular interaction prediction, authors commonly use classification
397 algorithms such as Support Vector Machine (SVM) [20], Random Forest (RF) [38], and K-
398 Nearest Neighbors (KNN). In our case, we used the Random Forest algorithm and determined
399 the hyperparameters using the grid search method. The optimal hyperparameters obtained are:

400 **Bootstrap:** True, **max_depth:** None, **min_samples_leaf:** 1, **min_samples_split:** 5,
401 **n_estimators:** 100.

402 6. Discussion

403 The results obtained in our study reveal better performance of our method for predicting
404 interactions between biological macromolecules. Through five-fold cross-validation, we
405 trained three distinct models, and the performances achieved, particularly for model 2,
406 demonstrate the efficiency of our approach. With a precision (PRE) of 99.29%, an accuracy
407 (ACC) of 99.52%, a recall (SEN) of 99.75%, an F1-score of 99.52%, and an area under the
408 ROC curve (ROC AUC) of 99.99%, our method significantly outperforms other techniques
409 compared in the literature. On average, the observed performances, with values of 98.83% for
410 precision, 99.4721% for accuracy, 98.83% for recall, 98.67% for F1-score, and 83.67% for
411 ROC AUC, confirm the robustness and effectiveness of our approach.

412 A comparison with commonly used feature extraction techniques in the literature, such as the
413 bi-gram method, DTI-BERT, BOW-GBDT, and DWKNN (Ensemble), highlighted the
414 superiority of our method. For instance, our approach achieves an accuracy rate of 99.52%,
415 surpassing the bi-gram, DTI-BERT, BOW-GBDT, and DWKNN (Ensemble) methods by
416 2.90%, 7.62%, 11.02%, and 14.42%, respectively. Similarly, for precision, our method
417 outperforms the other techniques by 3.90% to 12.18%. The Matthews Correlation Coefficient
418 (MCC) also shows an improvement ranging from 5.65% to 30.42%, depending on the method
419 compared. These results not only confirm the efficiency of our approach but also its ability to
420 better capture the complex interactions between biological macromolecules.

421 One of the main strengths of our approach lies in the optimized use of Random Forest,
422 combined with a particularly effective feature extraction method. Our feature extraction
423 method appears to better capture the relevant information from amino acid sequences
424 compared to other methods. Unlike models like DTI-BERT, which may require larger data
425 volumes for effective learning, our method seems more suitable even for moderately sized
426 datasets. The choice of Random Forest proved to be wise due to its ability to handle complex
427 datasets with nonlinear relationships. Moreover, the optimization of hyperparameters through
428 the grid search method allowed us to maximize the model's performance, making our method
429 not only precise but also robust and generalizable to other datasets.

430 Another key advantage of our method is its flexibility. Unlike methods like DTI-BERT, which
431 require substantial data volumes for optimal learning, our approach performs well even with
432 smaller datasets. This feature is particularly valuable in the context of predicting interactions
433 between biological macromolecules, where data can be limited.

434 Although our method shows exceptional overall performance, certain limitations deserve to
435 be discussed. The average value of the ROC AUC, although respectable at 83.67%, is lower
436 than the other metrics. This could suggest sensitivity to false positives or false negatives, an
437 aspect that could be improved in future work.

438 Furthermore, the complexity of the Random Forest model, although beneficial for precision,
439 can pose challenges in terms of computation time, especially during hyperparameter
440 optimization. Future research could explore alternative approaches to reduce this complexity
441 without sacrificing precision, such as integrating lighter ensemble learning techniques or
442 using more efficient feature selection methods.

443 **7. Conclusion**

444 In this study, we presented a new feature extraction method to predict interactions between
445 biological macromolecules. By generating feature vectors from macromolecule sequences
446 using a combination of bigram methods and pseudo-amino acid descriptors, our approach
447 demonstrated its effectiveness. The results obtained, with precision and accuracy rates
448 exceeding 99%, attest to the robustness and reliability of our method.

449 The superiority of our approach compared to traditional techniques lies in its ability to extract
450 relevant and representative information from macromolecule sequences, even from
451 moderately sized datasets. This flexibility, combined with the use of an optimized Random
452 Forest model, allowed us to maximize predictive performance while ensuring a high
453 generalization of results.

454 We can therefore conclude that our proposed extraction approach constitutes a significant
455 advancement in the field of molecular biology. It offers a practical and effective solution for
456 the analysis of macromolecular interactions, thereby contributing to the understanding of
457 fundamental biological processes and the development of new therapeutic applications.

458

459 8. References

- 460 [1] A. W. Senior et al., « Improved protein structure prediction using potentials from deep
461 learning », *Nature*, vol. 577, no 7792, Art. no 7792, janv. 2020, doi: 10.1038/s41586-019-1923-7.
- 462 [2] A. R. Jalalvand, « Chemometrics in investigation of small molecule-biomacromolecule
463 interactions: A review », *Int. J. Biol. Macromol.*, vol. 181, p. 478-493, juin 2021, doi:
464 10.1016/j.ijbiomac.2021.03.184.
- 465 [3] I. P. Gerothanassis, « Ligand-observed in-tube NMR in natural products research: A review on
466 enzymatic biotransformations, protein–ligand interactions, and in-cell NMR spectroscopy », *Arab. J.
467 Chem.*, vol. 16, no 3, p. 104536, mars 2023, doi: 10.1016/j.arabjc.2022.104536.
- 468 [4] U. Salar, Atia-tul-Wahab, et M. Iqbal Choudhary, « Biochemical evaluation and ligand binding
469 studies on glycerophosphodiester phosphodiesterase from *Staphylococcus aureus* using STD-NMR
470 spectroscopy and molecular docking analysis », *Bioorganic Chem.*, vol. 144, p. 107153, mars 2024,
471 doi: 10.1016/j.bioorg.2024.107153.
- 472 [5] W. Wang, S. Thiemann, et Q. Chen, « Utility of SPR technology in biotherapeutic
473 development: Qualification for intended use », *Anal. Biochem.*, vol. 654, p. 114804, oct. 2022, doi:
474 10.1016/j.ab.2022.114804.
- 475 [6] E. A. FitzGerald et al., « Multiplexed experimental strategies for fragment library screening
476 against challenging drug targets using SPR biosensors », *SLAS Discov.*, vol. 29, no 1, p. 40-51, janv.
477 2024, doi: 10.1016/j.slasd.2023.09.001.
- 478 [7] V. M. Patil, S. P. Gupta, N. Masand, et K. Balasubramanian, « Experimental and
479 computational models to understand protein-ligand, metal-ligand and metal-DNA interactions
480 pertinent to targeted cancer and other therapies », *Eur. J. Med. Chem. Rep.*, vol. 10, p. 100133, avr.
481 2024, doi: 10.1016/j.ejmcr.2024.100133.
- 482 [8] L. Zhang, D. Lu, X. Bi, K. Zhao, G. Yu, et N. Quan, « Predicting disease genes based on
483 multi-head attention fusion », *BMC Bioinformatics*, vol. 24, no 1, p. 162, avr. 2023, doi:
484 10.1186/s12859-023-05285-1.
- 485 [9] M. Romero, O. Ramírez, J. Finke, et C. Rocha, « Feature extraction with spectral clustering
486 for gene function prediction using hierarchical multi-label classification », *Appl. Netw. Sci.*, vol. 7, no
487 1, p. 28, déc. 2022, doi: 10.1007/s41109-022-00468-w.
- 488 [10] J. Costa-Silva, D. S. Domingues, D. Menotti, M. Hungria, et F. M. Lopes, « Computational
489 methods for differentially expressed gene analysis from RNA-Seq: an overview », 8 septembre 2021,
490 arXiv: arXiv:2109.03625. doi: 10.48550/arXiv.2109.03625.
- 491 [11] C. Heydt et al., « Detection of gene fusions using targeted next-generation sequencing: a
492 comparative evaluation », *BMC Med. Genomics*, vol. 14, no 1, p. 62, févr. 2021, doi: 10.1186/s12920-
493 021-00909-y.
- 494 [12] J. Wang et al., « MIFNN: Molecular Information Feature Extraction and Fusion Deep Neural
495 Network for Screening Potential Drugs », *Curr. Issues Mol. Biol.*, vol. 44, no 11, Art. no 11, nov. 2022,
496 doi: 10.3390/cimb44110382.
- 497 [13] X. Zhao et al., « PermuteDDS: a permutable feature fusion network for drug-drug synergy
498 prediction », *J. Cheminformatics*, vol. 16, no 1, p. 41, avr. 2024, doi: 10.1186/s13321-024-00839-8.

- 499 [14] W. Yang, Q. Zhou, M. Yuan, Y. Li, Y. Wang, et L. Zhang, « Dual-band polarimetric HRRP
500 recognition via a brain-inspired multi-channel fusion feature extraction network », *Front. Neurosci.*,
501 vol. 17, août 2023, doi: 10.3389/fnins.2023.1252179.
- 502 [15] B. M. Good et al., « Reactome and the Gene Ontology: digital convergence of data resources
503 », *Bioinformatics*, vol. 37, no 19, p. 3343-3348, oct. 2021, doi: 10.1093/bioinformatics/btab325.
- 504 [16] Q. Chen et al., « Network-based methods for gene function prediction », *Brief. Funct.*
505 *Genomics*, vol. 20, no 4, p. 249-257, juill. 2021, doi: 10.1093/bfpg/elab006.
- 506 [17] S. Rapposelli, E. Gaudio, F. Bertozzi, et S. Gul, « Editorial: Protein–Protein Interactions: Drug
507 Discovery for the Future », *Front. Chem.*, vol. 9, nov. 2021, doi: 10.3389/fchem.2021.811190.
- 508 [18] W. A. Abbasi, A. Yaseen, F. U. Hassan, S. Andleeb, et F. U. A. A. Minhas, « ISLAND: in-silico
509 proteins binding affinity prediction using sequence information », *BioData Min.*, vol. 13, no 1, p. 20,
510 nov. 2020, doi: 10.1186/s13040-020-00231-w.
- 511 [19] G. Czibula, A.-I. Albu, M. I. Bocicor, et C. Chira, « AutoPPI: An Ensemble of Deep
512 Autoencoders for Protein–Protein Interaction Prediction », *Entropy*, vol. 23, no 6, Art. no 6, juin 2021,
513 doi: 10.3390/e23060643.
- 514 [20] C. N. Kopoin, N. T. Tchimou, B. K. Saha, et M. Babri, « A Feature Extraction Method in
515 Large Scale Prediction of Human Protein-Protein Interactions using Physicochemical Properties into
516 Bi-gram », in *2020 IEEE International Conf on Natural and Engineering Sciences for Sahel’s*
517 *Sustainable Development - Impact of Big Data Application on Society and Environment (IBASE-BF)*,
518 Ouagadougou, Burkina Faso: IEEE, févr. 2020, p. 1-7. doi: 10.1109/IBASE-BF48578.2020.9069594.
- 519 [21] K.-C. Chou, « Using amphiphilic pseudo amino acid composition to predict enzyme subfamily
520 classes », *Bioinformatics*, vol. 21, no 1, p. 10-19, janv. 2005, doi: 10.1093/bioinformatics/bth466.
- 521 [22] R. Veevers et D. MacLean, « Improved K-mer Based Prediction of Protein-Protein Interactions
522 With Chaos Game Representation, Deep Learning and Reduced Representation Bias », 23 octobre
523 2023, arXiv: arXiv:2310.14764. Consulté le: 20 juin 2024. [En ligne]. Disponible sur:
524 <http://arxiv.org/abs/2310.14764>
- 525 [23] L. Rampásek, M. Galkin, V. P. Dwivedi, A. T. Luu, G. Wolf, et D. Beaini, « Recipe for a
526 General, Powerful, Scalable Graph Transformer », 15 janvier 2023, arXiv: arXiv:2205.12454.
527 Consulté le: 20 juin 2024. [En ligne]. Disponible sur: <http://arxiv.org/abs/2205.12454>
- 528 [24] G. Wang et al., « Deep-learning-enabled protein–protein interaction analysis for prediction of
529 SARS-CoV-2 infectivity and variant evolution », *Nat. Med.*, vol. 29, no 8, p. 2007-2018, août 2023,
530 doi: 10.1038/s41591-023-02483-5.
- 531 [25] L. Xian et Y. Wang, « Advances in Computational Methods for Protein–Protein Interaction
532 Prediction », *Electronics*, vol. 13, no 6, Art. no 6, janv. 2024, doi: 10.3390/electronics13061059.
- 533 [26] F. Soleymani, E. Paquet, H. Viktor, W. Michalowski, et D. Spinello, « Protein–protein
534 interaction prediction with deep learning: A comprehensive review », *Comput. Struct. Biotechnol. J.*,
535 vol. 20, p. 5316-5341, sept. 2022, doi: 10.1016/j.csbj.2022.08.070.
- 536 [27] H.-N. Tran, P.-X.-Q. Nguyen, F. Guo, et J. Wang, « Prediction of Protein–Protein Interactions
537 Based on Integrating Deep Learning and Feature Fusion », *Int. J. Mol. Sci.*, vol. 25, no 11, Art. no 11,
538 janv. 2024, doi: 10.3390/ijms25115820.
- 539 [28] L. Hu, X. Wang, Y.-A. Huang, P. Hu, et Z.-H. You, « A survey on computational models for
540 predicting protein–protein interactions », *Brief. Bioinform.*, vol. 22, no 5, p. bbab036, sept. 2021, doi:
541 10.1093/bib/bbab036.

- 542 [29] X. Hu, C. Feng, T. Ling, et M. Chen, « Deep learning frameworks for protein–protein
543 interaction prediction », *Comput. Struct. Biotechnol. J.*, vol. 20, p. 3223-3233, janv. 2022, doi:
544 10.1016/j.csbj.2022.06.025.
- 545 [30] F. Soleymani, E. Paquet, H. L. Viktor, W. Michalowski, et D. Spinello, « ProtInteract: A deep
546 learning framework for predicting protein–protein interactions », *Comput. Struct. Biotechnol. J.*, vol.
547 21, p. 1324-1348, janv. 2023, doi: 10.1016/j.csbj.2023.01.028.
- 548 [31] C. Chen et al., « Improving protein-protein interactions prediction accuracy using XGBoost
549 feature selection and stacked ensemble classifier », *Comput. Biol. Med.*, vol. 123, p. 103899, août
550 2020, doi: 10.1016/j.combiomed.2020.103899.
- 551 [32] X. Du, S. Sun, C. Hu, Y. Yao, Y. Yan, et Y. Zhang, « DeepPPI: Boosting Prediction of Protein–
552 Protein Interactions with Deep Neural Networks », *J. Chem. Inf. Model.*, vol. 57, no 6, p. 1499-1510,
553 juin 2017, doi: 10.1021/acs.jcim.7b00028.
- 554 [33] C. Malbranke, W. Rostain, F. Depardieu, S. Cocco, R. Monasson, et D. Bikard, «
555 Computational design of novel Cas9 PAM-interacting domains using evolution-based modelling and
556 structural quality assessment », *PLOS Comput. Biol.*, vol. 19, no 11, p. e1011621, nov. 2023, doi:
557 10.1371/journal.pcbi.1011621.
- 558 [34] W.-R. Qiu, A. Xu, Z.-C. Xu, C.-H. Zhang, et X. Xiao, « Identifying Acetylation Protein by
559 Fusing Its PseAAC and Functional Domain Annotation », *Front. Bioeng. Biotechnol.*, vol. 7, déc.
560 2019, doi: 10.3389/fbioe.2019.00311.
- 561 [35] Åbo Akademi University, Faculty of Social Sciences, Business and Economics, Turku,
562 Finland, L. Davoodi, J. Mezei, et Åbo Akademi University, Faculty of Social Sciences, Business and
563 Economics, Turku, Finland, « A Comparative Study of Machine Learning Models for Sentiment
564 Analysis: Customer Reviews of E-Commerce Platforms », in *35 th Bled eConference Digital
565 Restructuring and Human (Re)action*, University of Maribor Press, 2022, p. 217-231. doi:
566 10.18690/um.fov.4.2022.13.
- 567 [36] A. Hernandez-Guedes, I. Santana-Perez, N. Arteaga-Marrero, H. Fabelo, G. M. Callico, et J.
568 Ruiz-Alzola, « Performance Evaluation of Deep Learning Models for Image Classification Over Small
569 Datasets: Diabetic Foot Case Study », *IEEE Access*, vol. 10, p. 124373-124386, 2022, doi:
570 10.1109/ACCESS.2022.3225107.
- 571 [37] P. Wang, X. Huang, W. Qiu, et X. Xiao, « Identifying GPCR-drug interaction based on
572 wordbook learning from sequences », *BMC Bioinformatics*, vol. 21, no 1, p. 150, avr. 2020, doi:
573 10.1186/s12859-020-3488-8.
- 574 [38] W. Qiu, Z. Lv, Y. Hong, J. Jia, et X. Xiao, « BOW-GBDT: A GBDT Classifier Combining
575 With Artificial Neural Network for Identifying GPCR–Drug Interaction Based on Wordbook Learning
576 From Sequences », *Front. Cell Dev. Biol.*, vol. 8, févr. 2021, doi: 10.3389/fcell.2020.623858.
- 577 [39] J. Zheng, X. Xiao, et W.-R. Qiu, « DTI-BERT: Identifying Drug-Target Interactions in Cellular
578 Networking Based on BERT and Deep Learning Method », *Front. Genet.*, vol. 13, juin 2022, doi:
579 10.3389/fgene.2022.859188.
- 580 [40] A. W. Senior et al., « Improved protein structure prediction using potentials from deep
581 learning », *Nature*, vol. 577, no 7792, Art. no 7792, janv. 2020, doi: 10.1038/s41586-019-1923-7.
- 582